1. Agency Use Only *(Leave blank).*	2. Report Date. October 1991	3. Report Type and Dates Covered. Final - Proceedings

4. Title and Subtitle.
Large Resonance Signatures in Scattering from Submerged Elastic Targets in the Time and Frequency Domain

5. Funding Numbers.

Contract	
Program Element No.	0601153N
Project No.	03202
Task No.	350
Accession No.	DN255011
Work Unit No.	12211B

6. Author(s).
M. F. Werby and S. A. Chin-Bing

7. Performing Organization Name(s) and Address(es).
Naval Oceanographic and Atmospheric Research Laboratory
Ocean Acoustics and Technology Directorate
Stennis Space Center, MS 39529-5004

8. Performing Organization Report Number.
PR 91:100:221

9. Sponsoring/Monitoring Agency Name(s) and Address(es).
Naval Oceanographic and Atmospheric Research Laboratory
Basic Research Management Office
Stennis Space Center, MS 39529-5004

10. Sponsoring/Monitoring Agency Report Number.
PR 91:100:221

11. Supplementary Notes.
Published in IEEE Oceans

12a. Distribution/Availability Statement.
Approved for public release; distribution is unlimited.

12b. Distribution Code.

13. Abstract *(Maximum 200 words).*

There are a variety of resonances that can be excited when one scatters a wave from a submerged elastic target. It is usual to detect these resonances by observing the backscattered echoes from either pulses for the time domain case or by varying frequency in small step sizes in the frequency domain case. Many such resonances produce fairly small effects that can get lost in the background in any realistic environment. On the other hand several types of resonances are quite prominent and quite possible can be observed even in a fluctuating environment. Many of these resonances have characteristic return signals and offer a "tell-tale" event of a particular target. We refer to such characteristic signals as "resonance signature." In this study we illustrate a number of "resonance signatures" and describe the underlying physics or mathematics behind the event. We indicate how these signatures can be useful in target identification.

14. Subject Terms.
Acoustic scattering, shallow water, waveguide propagation

15. Number of Pages.
9

16. Price Code.

17. Security Classification of Report.	18. Security Classification of This Page.	19. Security Classification of Abstract.	20. Limitation of Abstract.
Unclassified	Unclassified	Unclassified	SAR

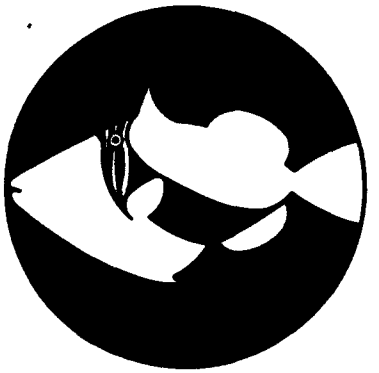

OCEANS 91

October 1-3, 1991 • Honolulu, Hawaii USA

Proceedings • Volume 3

Ocean Technologies and Opportunities in the Pacific for the 90's

Sponsored by the Oceanic Engineering Society of IEEE

91CH3063-5

LARGE RESONANCE SIGNATURES IN SCATTERING FROM SUBMERGED ELASTIC TARGETS IN THE TIME AND FREQUENCY DOMAIN

M. F. Werby and S. A. Chin-Bing

Naval Oceanographic and Atmospheric Research Laboratory
Acoustic Theory and Simulation Branch, Code 221
Stennis Space Center, MS 39529-5004

Abstract

There are a variety of resonances that can be excited when one scatters a wave from a submerged elastic target. It is usual to detect these resonances by observing the backscattered echoes from either pulses for the time domain case or by varying frequency in small step sizes in the frequency domain case. Many such resonances produce fairly small effects that can get lost in the background in any realistic environment. On the other hand several types of resonances are quite prominent and quite possibly can be observed even in a fluctuating environment. Many of these resonances have characteristic return signals and offer a "tell-tale" event of a particular target. We refer to such characteristic signals as "resonance signatures." In this study we illustrate a number of "resonance signatures" and describe the underlying physics or mathematics behind the event. We indicate how these signatures can be useful in target identification.

1. Introduction

Resonances are excited by incident acoustical signals as they impinge on elastic bodies of rotation as well as elastic bars. They are characterized by the fact that they occur at discrete values of frequency and when they occur, a characteristic event takes place. This event can be complicated and difficult to distinguish from other physical mechanisms unrelated to resonances but they are usually distinguishable and can be related to a particular process. Recent theoretical and numerical developments[1-21] have enabled researchers to perform calculations and to understand the nature of resonances. Our interest in this paper is to investigate particularly large and distinguishable resonances that manifest themselves in either the frequency or time domain. In the literature there have been three classes of resonances usually studied. Investigations of Lamb resonances due to symmetric and antisymmetric waves (labeled S_i and A_i for i = 0,1,2, . . .) for shells[2-4,15,18-20] have been vigorously investigated; for elastic solids, Rayleigh resonances (labeled as an ordered pair (n,1) with n = 2,3,4 . . .) and whispering gallery resonances (labeled as an ordered pair (n,l) with n = 0,1,2 . . . and l = 2,3,4 . . .) have also been extensively studied.[1,9,10-12,17,21] Here n corresponds to the mode number of the resonance viewed as a surface standing wave with n = 0 corresponding to a breathing mode. These resonances are not particularly pronounced in magnitude or signature (the characteristic shape of the resonance). In this work we wish to examine classes of resonances that are somewhat more pronounced in magnitude or pattern either in the time or frequency domains. We will give a brief discussion of these phenomena including effects peculiar to spheroids such as orthogonal classes of resonances recently discussed in the literature.[15,21] However, emphasis will be placed on the following: 1) resonances at coincident frequency (the frequency at which the speed of the flexural Lamb wave equals the speed of sound in the fluid) excited on submerged elastic shells; 2) "resonances" due to high frequency incident plane waves on a submerged elastic shell due to an internal reflection effect; and 3) flexural or bending resonances due to plane oblique incident waves on a spheroid. It will be seen that each of these classes of resonances are rather large, have characteristic signatures and have locations predictable using simplified expressions. In the time-domain case a recently advanced methodology arising from a time-domain resonance scattering theory is used to discuss the existence of strong pseudo-Stonely resonances excited on elastic shells that give rise to a strong beat pattern in the time-domain resonance signature. The time-domain methodology is outlined below. However, since we will have occasion to use the correct acoustical background for an elastic shell this recent development[22] will be outline in the next section.

2. A New Acoustic Background for Submerged Elastic Shells

The rigid background concept for elastic solid targets in which the total elastic response is viewed as a superposition of a resonance response and a nonresonant acoustical background[1] (rigid for solid elastic targets) has proven quite successful as the "correct" background for elastic solids submerged in water. An analogous background for the elastic shell problem has proven more elusive to find. Earlier work[2-4] has shown that for very thin shells a soft background is useful in extracting the elastic residual, but for shells of greater thickness and at high frequencies, a rigid background has proven suitable. It has also been demonstrated that for some cases a soft background was suitable at the lower frequency limit and that a rigid background was suitable at the higher frequency limit for the same target. The Überall group[4] at the Catholic University of America has employed a rigid background for elastic shells with some success for very thick shells. In this paper a model is discussed that describes acoustic scattering from an elastic shell in the absence of resonances. We then demonstrate that it is a suitable background for the elastic shell problem by presenting numerous examples that manifest a pure residual resonance response.

The model is then applied over a ka range from 0 to 300 for steel and WC at a thickness of 1%, and for steel at thicknesses of 0.3% (i.e., ratios of inner-to-outer radii of 0.99 and 0.997) with highly satisfactory results.

The inertial component of the radiation loading of a spherical shell at the surface is in the form:[5]

$$P_s = -i\omega \sum_{i=0}^{\infty} M_n \dot{W}_n P_n^0(1), \tag{1}$$

where $M_n = -\frac{\rho}{k} \mathrm{Im}\left(i \frac{h_n(ka)}{h'_n(ka)} \right)$.

Here, M_n is the entrained mass per unit area for mode n, ω is the angular frequency, ρ the density of a fluid, $P_n^0(1)$ is an associated Legendre polynomial evaluated at 180 degrees, k is the wave number, and h_n is an outgoing spherical Hankel Function. Here $\dot{W}_n$ is an expansion coefficient related to the displacement potential. If we excite the sphere by an incident monochromatic plane wave, then we have

$$\dot{W}_n = -i\omega\, a_n(j_n(ka) + b_n h_n(ka))\exp(-i\omega t),$$

where j_n is a regular Bessel function and b_n is an unknown coefficient which corresponds to the partial wave scattering amplitude which we seek. Here, a_n is the plane wave expansion coefficient. The total pressure per unit area in the fluid due to the incident plane wave is

$$P_t = \frac{\rho c \omega}{ka} \sum_{n=0}^{\infty} a_n \left(j_n(kr) + b_n h_n(kr) \right) P_n^0(1) \exp(-i\omega t). \tag{2}$$

The particle velocity at the surface of the object is: $v = -\frac{-i}{\rho \omega k} \frac{\partial P_t}{\partial r}$.

Here, c is the speed of sound in water. The particle acceleration α is the time derivative of v which leads to:

$$\alpha = -\frac{\omega^2}{ka} \sum_{n=0}^{\infty} a_n \left(j'_n(kr) + b_n h'_n(kr) \right) P_n^0(1) \exp(-i\omega t). \tag{3}$$

0-7803-0202-8/91/0000-1352$1.00©1991 IEEE

The force at the surface of the object due to the incident plane wave is simply the product of the particle acceleration and the mass of the spherical shell. The mass of the spherical shell is $4\pi\rho_s a^3[1-(1-h)^3]/3$, where h is the ratio of the shell thickness to the shell radius. The force due to the total fluid loading at the object surface is equal to the total inertial fluid loading times the surface area $4\pi a^2$ of the sphere. Here, a is the radius of the spherical shell and ρ_s is the density of the shell material. We equate these two forces to obtain the unknown coefficient b_n which leads to the following expression.

$$b_n = -\frac{\frac{3\rho}{\rho_s\left[1-(1-h)^3\right]}\,\mathrm{Im}\left(i\frac{h_n(ka)}{h'_n(ka)}\right)j_n(ka)-j'_n(ka)}{\frac{3\rho}{\rho_s\left[1-(1-h)^3\right]}\,\mathrm{Im}\left(i\frac{h_n(ka)}{h'_n(ka)}\right)h_n(ka)-h'_n(ka)} \qquad (4)$$

The scattered field for the new background is obtained by using the b_n's as the partial wave scattering amplitudes in a normal mode series. The b_n's define the new background and by subtracting this quantity from the elastic response, we obtain the residual response that reflects mainly the pure resonance contribution. It is easy to show that the imaginary part of the enclosed brackets in Eq. 4 is approximately equal to $ka/(1+ka^2)$ so that for large ka, $b_n = -j'_n(ka)/h'_n(ka)$ which corresponds to a rigid scatterer and for both a very thin shell and at low frequency, $b_n = -j_n(ka)/h_n(ka)$ which corresponds to a soft scatterer. Thus we see that the background represented by Eq. 4 has the appropriate limits for thin shells at low frequencies (soft) as well as the appropriate limits for high frequencies (rigid).

2.1 Application to Elastic Shells

In an earlier work, the form function due to an incident plane wave on a steel spherical shell with thickness 0.3% of the radius was examined.[3] Figure 1a is the form function for the shell for a ka range between 0 and 300. At the lower frequency end, a soft background appeared adequate but at quite high frequencies, a rigid background appeared adequate; intermediate regions were poorly represented by both backgrounds. In Fig. 1b and Fig. 1c a soft and rigid background are subtracted (in partial wave space) to illustrate that only at the extreme ends does either background appear adequate. Figure 1d illustrates the case for which the new background is subtracted from the form function and it is evident that it is superior for the entire region of ka. Figure 2a–2d illustrates the same example for a shell of 1% thickness (the form function, the residual obtained by subtracting soft, the residual obtained by subtracting rigid, and the residual obtained by subtracting the new background). Again, it is evident from Fig. 2 that the new background is indeed adequate even in the region of strong flexurals around ka = 120.

Figure 3a–3d illustrates plane wave scattering from 1% thick WC shells for the elastic response (3a), the elastic response minus the soft background (3b), the elastic response minus the rigid background (3c), and the elastic response minus the new background (3d). For the WC case the new background is also quite superior to the others. In contrast to aluminum, the rigid background is adequate over a larger range due to the high density of WC, as predicted by Eq. 4. Further, the isolation of resonances at the higher ka region is superior to either steel or aluminum; the explanation is presented in the next section.

3. Time Domain Resonance Scattering Theory

The partial wave series that emerges from normal mode theory for separable geometries can be represented in distinct partial waves or modes. It has been shown[1,17] that a representation due to a distinct mode {n} can be written in the form:

$$f_n(\theta) = \frac{2}{ka}e^{2i\xi_n^{(r)}}\left\{\frac{\left(\frac{1}{2}\right)s\Gamma_n^{(r)}}{\chi-\chi_n^{(r)}+\left(\frac{i}{2}\right)\Gamma_n^{(r)}}+e^{-i\xi_n^{(r)}}\sin\xi_n^{(r)}\right\} \qquad (5)$$

where $c = ka$, $\chi_n^{(r)}$ is the nth resonance and $\left(\frac{1}{2}\right)\Gamma_n^{(r)}$ the half-width.

Where $e^{2i\xi_n^{(r)}} = -\dfrac{h_n^{(2)'}(x)}{h_n^{(1)'}(x)}$.

Here, the factor $2n+1$ is absorbed in the expansion coefficient. For the pulse form a continuous wave (cw) ping is used which corresponds

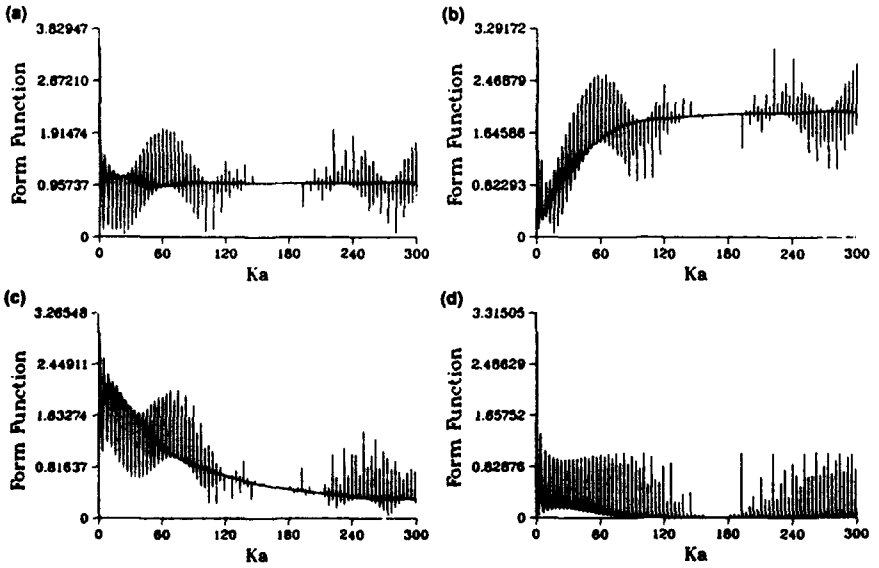

Figure 1. Scattering response for ka = 0 to 300 for 0.3% steel shell, (a) total response; (b) total minus soft background; (c) total minus rigid background; and (d) total minus new background.

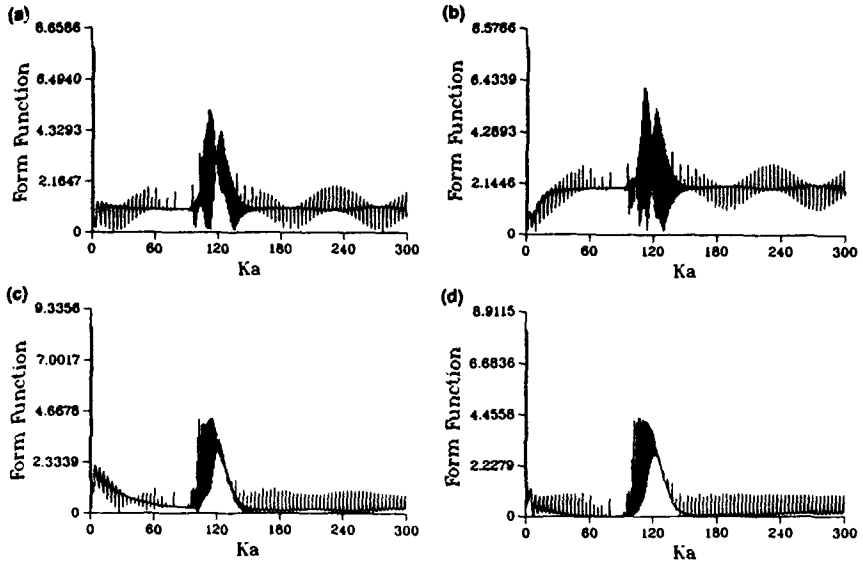

Figure 2. Scattering response for ka = 0 to 300 for 1% thick shell, (a) total response; (b) total minus soft background; (c) total minus rigid background; and (d) total minus new background.

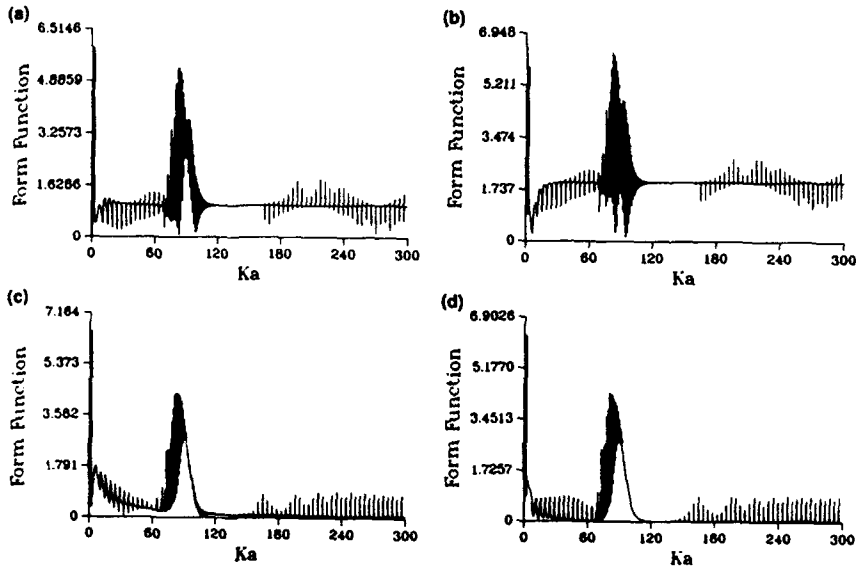

Figure 3. Scattering response for ka = 0 to 300 for 1% thick WC, (a) total response; (b) total minus soft background; (c) total minus rigid background; and (d) total minus new background.

to a very broad frequency range. For each time domain modal component, one has that

$$\mathrm{Re}\int_{-\infty}^{\infty} \frac{\left(\frac{1}{2}\right)\Gamma_n^{(r)}}{\chi-\chi_n^{(r)}+\left(\frac{i}{2}\right)\Gamma_n^{(r)}} e^{-ixs}\,dx = 2\pi\left(\frac{1}{2}\right)\Gamma_n^{(r)}\sin\left(\chi_n^{(r)}s\right)e^{-\left(\frac{1}{2}\right)s\Gamma_n^{(r)}} . \quad (6)$$

That is, at a resonance the time-domain solution is simply the product of the half-width times a sinusoidal function times an exponential damping factor. From the time-domain solution for a nest of resonances (N-m) for a cw ping, one obtains the form

$$P(s) = 2\pi \sum_{n=m}^{N} \left(\frac{1}{2}\right)\Gamma_n^{(r)}\sin\left(\chi_n^{(r)}s\right)e^{-\left(\frac{1}{2}\right)s\Gamma_n^{(r)}} . \quad (7)$$

The remaining contributions from backscatter are small due to phase averaging.

It is assumed that calculations are performed in a resonance region for which the resonance widths are fairly constant and the resonance spacing is fairly uniform.[19,20] This assumption leads to the important expression

$$P(s) = 2\pi 2^M \left|\sin\left(\chi_{ave}^{(r)}s\right)\right| \left|\cos\left(\Delta\chi_{ave}^{(r)}s/2\right)\right|^M e^{-s\Gamma/2} , \quad (8)$$

where $\chi_{ave}^{(r)} = \frac{1}{2M}\sum_{i=n}^{n+2M}\chi_i^{(r)}$.

Here one sets n – m = 2M. It is seen from the above expression:

– The half-width is associated with the decay of the response in the

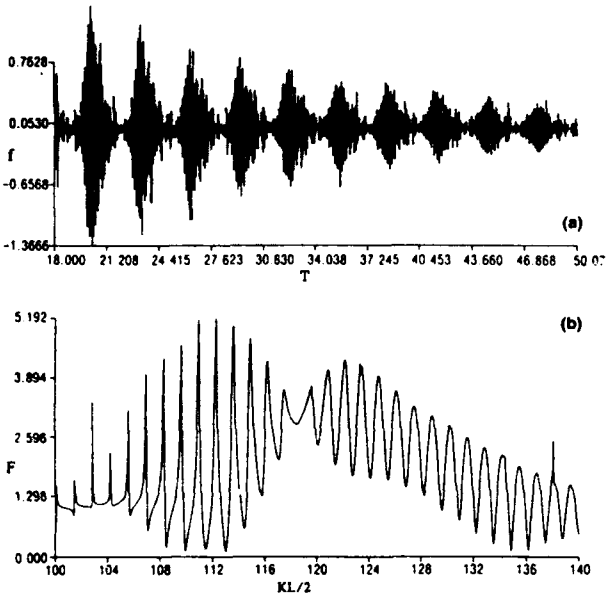

Figure 4. (a) Time domain; and (b) frequency domain for scattering from a steel shell of 1% thickness about coincidence frequency.

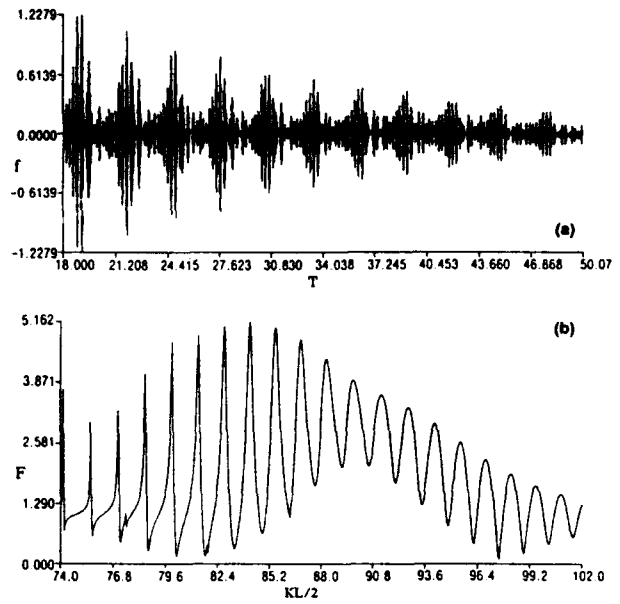

Figure 5. (a) Time domain; and (b) frequency domain for scattering from a WC shell of 1% thickness about coincidence frequency.

time domain solution: the response decreases exponentially with increasing value of the half-width.

– When the number of adjacent resonances (2M) sensed increases, the return signal becomes more sharply defined and the envelope function (the beats) are more enhanced and clearly defined.

– For larger carrier frequencies, the signal is more oscillatory within the envelope.

3.1 Time Domain Backscattering at Coincidence Frequency

Flexural waves do not yield resonances from fluid-loaded shells until the phase velocity of the flexural wave is about equal to the speed of sound in the ambient fluid.[5,24] The value in frequency for which this happens is referred to as the coincidence frequency; however, some subsonic fluid-borne waves produce sharp resonances[19,20] below coincidence frequency. These waves are referred to as pseudo-Stonely waves and the related resonances as pseudo-Stonely resonances.[20] The pseudo-Stonely resonances are well defined in partial wave space; they usually correspond to only one partial wave mode number and a very narrow half-width with a dispersive phase velocity, which approaches the speed of sound in the fluid with increasing frequency. The pseudo-Stonely resonances diminish in significance at the point where the flexural resonances begin to dominate. It can be determined that a phase change occurs in the pressure field in the transition region from subsonic to supersonic. This change accounts for the envelope of the resonance curve at coincidence frequency where the waves are in phase until coincidence and are out of phase afterwards. Our interest here is in examining the time-domain response since one expects the conditions previously described to be partially met over a broad frequency range and thus to yield a strong coherent response with a carrier frequency in the neighborhood of the frequency at coincidence. Accordingly, the case of cw pings for two examples—for which coincidence resonances are expected to arise—is examined. This is certainly suggested by the strong responses in Figs. 4b and 5b at the ka values 113 and 87, respectively, for steel and WC. Further, in this analysis the Mindlin-Timoshenko[24] thick plate theory is used to determine the value for which the flexural phase velocity will equal the ambient speed of sound in water. The phase and group velocities are determined from flat plate theory which proves to be quite reliable in predicting the phase velocity for the curved surfaces of the spheres at the coincidence frequency.

The time-domain calculations are now examined. The first example is a steel shell of 1% thickness. In this case a well-defined envelope (illustrated in Fig. 4a) with pronounced oscillations within the envelope is consistent with Eq. 8. The enhancement due to the factor 2^M is obvious both here and in Fig. 5a for the WC case. The group velocity can be obtained from the peak-to-peak distance of the adjacent envelopes. The result leads to a value of 2.23 km/sec. Both flexural and pseudo-Stonely resonances compete in this region. A mixture of pseudo-Stonely waves, as well as flexural waves must be leaking into the fluid. For flexural waves, the group velocity is 2.53 km/sec at coincidence frequency with a range between 2.44 and 2.68 km/sec over the ka range of 100-140, where the strong flexurals are significant. In that range the phase velocity varies from 1.37 to 1.58 km/sec. The value of the extracted group velocity does not agree well with the flexural group velocity; the discrepancy is 12%. This variation suggests that the flexural resonances are of little importance for the time sequence presented here. The group velocity of the pseudo-Stonely waves for this case has been determined[19] to be 2.16 km/sec based on plate theory. The phase velocity is in the range from 88% to 98% of the speed of sound in the fluid. This value of group velocity is within 3% of the extracted value from the time-domain solution. Moreover, the pseudo-Stonely resonances have very narrow widths while the flexural resonances are quite large. The conditions in the previous section would indicate that the flexural resonances would rapidly dampen due to the large half-widths while the pseudo-Stonely resonances would attenuate slowly in time. Thus, based on the similarity of the extracted group velocity and that of the pseudo-Stonely wave and the conditions in the previous section on level widths, one may conclude that the time-domain calculations in Fig. 4a represent pseudo-Stonely resonances.

The final example is for the WC shell of 1% thickness. The results of the calculation are consistent with that of the steel case and are illustrated in Fig. 5b. Here the group velocity was extracted to be 2.33 km/sec as opposed to the plate theory value of 2.65 km/sec for flexural waves. The range of values for the group velocities predicted was from 2.49 to 2.78 km/sec over the ka ranging from 74 to 102. Here, as in the previous example, the difference was 12% between the extracted value and the value predicted for flexural waves. The group velocity for pseudo-Stonely waves is, however, 2.26 which is within 3% of the extracted value here. As in the previous example the pseudo-Stonely resonances are quite narrow and the flexural resonances are broad and one may conclude that the results of Fig. 5b represent pseudo-Stonely resonances. Further, we use Mindlin-Timoshenko[24] thick plate

theory to determine the value for which the flexural phase velocity will equal the ambient speed of sound in water. The expressions we use are from flat plate theory but they prove to be quite reliable in predicting the phase velocity for the curved surfaces of the spheres at the frequency limits in the vicinity of the value at coincidence frequency. It is remarkable that they in fact do predict the frequency range in the figures which match the strong flexurals. We determine that the expression for the phase velocity is:

$$v_f = \frac{v_p\left[\left\{(\Gamma-1)^2\left(\frac{\omega}{\Omega}\right)^4 + 4\left(\frac{\omega}{\Omega}\right)^2\right\}^{1/2} - (\Gamma+1)\left(\frac{\omega}{\Omega}\right)^2\right]^{1/2}}{\left[2\left(1-\Gamma\left(\frac{\omega}{\Omega}\right)^2\right)\right]^{1/2}} \qquad (9)$$

where $\Omega = \frac{C_p\sqrt{12}}{h}$ $\Gamma = 2.65\ (1 + 1.5\nu + 0.75\nu^2)$

and $\frac{\omega}{\Omega} = \frac{(ka)V_w\left(\frac{h}{a}\right)}{C_p\sqrt{12}}$

and $C_p = C_s\sqrt{\frac{2}{1-\nu}}$.

Here C_s is the shear speed and ν is the Poisson ratio of the material. The ratio (h/a) is a thickness parameter and V_w is the speed of sound in water. The remaining defining expressions in Eq. 10 are discussed in Ref. 24. For the cases presented here, (h/a) is 0.01 where a is the radius of the sphere. The group velocity is determined by us to be:

$$\frac{d\omega}{dk} = \frac{\left[2C_p^2 - (\Gamma+1)v_f^2\right]\left(\frac{\omega}{\Omega}\right)^2}{12v_f^3 C_p^2 + \left\{(\Gamma+1)C_p^2 v_f - 2\Gamma v_f^3\right\}\left(\frac{\omega}{\Omega}\right)^2}. \qquad (10)$$

Equation 10 was used to predict the group velocity reported in this work.

4. Thickness Effects Due to Internal Reflections From a Shell at High Frequency

If one scatters a plane wave from an elastic shell then at a frequency at which the interior wave length (associated with the compressional velocity of the material) is equal to an integral value of the thickness, then it can be shown that the shell will appear transparent to the signal. Consequently the signal will reflect off of the inner surface of the shell and add coherently with the specular signal at detection. For evacuated shells this tends to produce a maximum at such values and, indeed, results that follow substantiate this. While this result is not properly a "resonance" in the sense of the other processes discussed here, for want of a better term we will refer to this rather large response as a resonance. It can also be shown that the upper value of ka at which this process takes place for a given thickness and multiple of a half integral, terminates with the lowest partial wave allowed. Thus, an examination of the partial waves at the lowest mode can substantiate that our interpretation of this phenomena is correct. That will be illustrated in the next section.

4.1 Thickness "Resonances" From Elastic Shells at High Frequency

Figure 6a and b are the form functions due to an incident plane wave on a spherical shell of 10% and 2.5% thickness for steel shells respectively. It is evident that in the region between about a ka = 120 and 490, there are rather pronounced returns which are quite a bit larger in amplitude then usually observed for symmetric and antisymmetric resonances. The explanation for this event is determined from the fact that when a wave goes into a layered material, if the wave length of the layer is equal to half the wavelength of the penetrating wave, the reflection coefficient is just equal to that due to the interior layers. In this case, this corresponds to a soft scatterer (the inclusion was evacuated) and thus the reflected signal when added to the usual surface reflected signal is at a maximum. We examine at what value of ka this will happen for a steel shell with compressional speed 5.95 km/sec. The relation due to a flat plate approximation (adequate at high frequency) is:

$$ka = \frac{n\pi c_l}{\frac{h}{a}c_w} \qquad n = 1, 2, 3 \ldots \qquad (11)$$

Here C_l and C_w are the compressional speed of sound for steel and water respectively (5.95 km/sec and 1.4825 km/sec) and h/a is the ratio of the thickness to the radius of the shell (here 0.1 and 0.025). Thus ka = 126 and 504, respectively, which are in the range of the large returns. Figure 7a–7c are the form functions of steel, molybdenum and WC for 5% thick shells. Here the compressional velocities are 5.95, 6.35 and 6.95 which are predicted (in the correct ranges) from Eq. 11. To determine that this is indeed the correct interpretation we examine where the plot is a maximum for the zeroth partial wave corresponding best to the flat plate approximation. Figure 8a–8c illustrates that this, indeed, is at ka = 126, 252 and 504, respectively for the steel cases. Moreover, Fig. 9a and 9b for the lowest partial waves yield similar agreement for molybdenum and WC. The broad width of the resonances is due to the fact that the thickness that the plane incident wave 'sees' the shell is usually greater then the shell thickness and must correspond to higher order partial waves but lower ka values. This interpretation also predicts higher order resonances (when the thickness is equal to a multiple of half-integrals) and, indeed, the predictions are corroborated and will be illustrated elsewhere.

5. Rayleigh, Lamb and Flexural Resonances

We will discuss flexural or bending resonances excited on a spheroid, and for contrast, briefly discuss the more well known resonances due to the generation of Rayleigh waves on an elastic solid and Lamb waves on elastic shells. Rayleigh, or rather leaky-Rayleigh-type, resonances are generated when incident plane waves impinge upon fluid loaded elastic solids of rotation such as spheres and spheroids. They correspond to frequencies at which the Rayleigh waves have half integral wave lengths on the object surface (this does not preclude

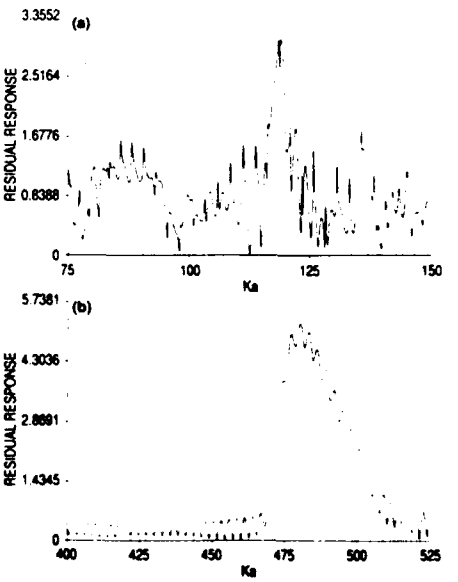

Figure 6. Form function for (a) 10%; and (b) (2.5% steel shell and thickness resonance.

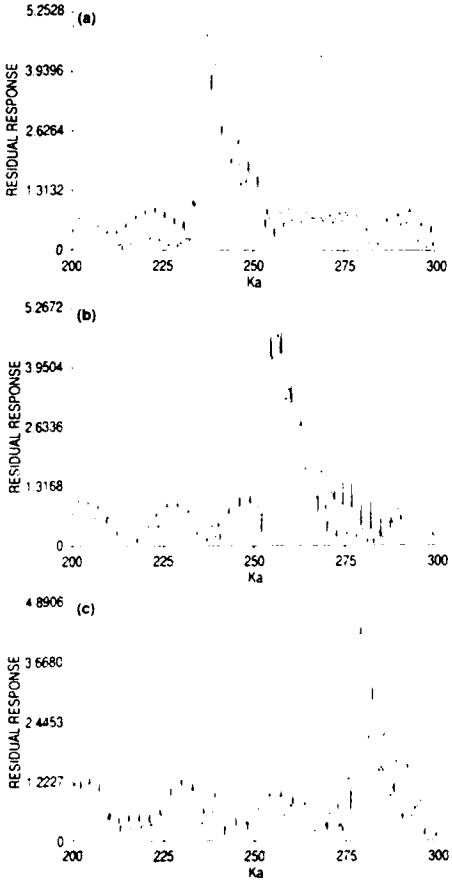

Figure 7. Form function for 5% thick shell and thickness resonance, (a) steel shell; (b) Molybdenum shell, and (c) WC shell.

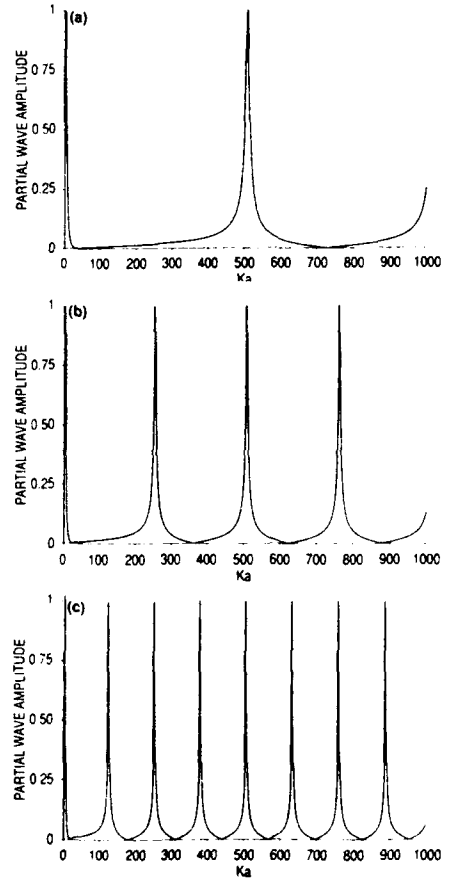

Figure 8. The lowest PWF for (a) 2.5%; (b) 5%; and (c) 10% steel shell to a Ka = 1000.

interior contributions of the waves) thus producing standing waves on the surface which in turn radiates back into the fluid. The extended boundary condition (EBC) method[6-14] offers one the possibility to predict such resonances. Lamb resonances are the analogue for shells in which it is possible to excite both symmetric (extensional) and antisymmetric (flexural) resonances.[16] The bending or flexural resonances (flexurals in this context are not to be confused with antisymmetric Lamb modes) occur on elongated objects such as spheroids both for solids and shells and can be modeled using the approximate theory of rods due to Timoshenko.[23]

We now examine a phenomenon specific to elastic objects with smooth boundary conditions surrounded by an acoustic fluid, namely, body resonances. The body resonances examined originate from the curved-surface equivalents of seismic interface waves of pseudo-Rayleigh or Scholte type, propagating circumferentially to form standing waves on a bounded object. If phase velocities are slowly-varying (as a function of frequency) at the object surface, resonances occur at discrete values of kL/2. These resonances manifest themselves in a prescribed manner (described below). For elongated elastic solids, three distinct resonance types occur. The first kind that we wish to illustrate has to do with bending modes or flexural resonances. For unsupported spheroids a plane incident wave at 45 degrees relative to the axis of symmetry can excite these modes. This is illustrated in Fig. 10 for aspect ratios of 4 and 5 to 1. It can be shown that the lowest mode corresponds to 2, and thereafter 3, 4, etc. The interesting thing about these resonances is they can be predicted by exact bar theories and coincide nicely with results here. Of particular interest is the effect that with increasing aspect ratio the onset of resonances occur at lower kL/2 values, the opposite observed for Rayleigh resonances. The resonances predicted for aspect ratios of 3, 4, and 5 are illustrated in Fig. 11a–11c. The modal pattern is illustrated in Fig. 12 for the first four modes. The second kind (at lower frequencies) are due to leaky Rayleigh waves and have been shown to be related to both target geometry and material parameters (notably shear modules and density). Resonances can in this case best be observed by examining the backscattered echo amplitude and phase response plotted as a function of kL/2, often referred to in the acoustic scattering literature as a form function. We illustrate this in Fig. 13, for broadside scattering from spheroids of aspect ratio 2, 3, 4, and 5. Here we see two resonances superimposed on the semi-periodic pattern due to Franz waves associated with rigid scattering. If we subtract rigid scattering (in partial wave space) from the elastic response, then we are left with the resonance response. In addition to the above wave phenomena, it is also possible to excite "whispering gallery" resonances, which can be seen for the lowest aspect ratio cases in Fig. 13. In Fig. 13, the parallel sign indicates that the resonances are excited about the longest meridian, while the perpendicular sign indicates that the resonance is excited about the shortest meridian. The fact that broadside incident plane waves do excite resonances not only about the shortest meridian, but also about the longest meridian—coinciding to the resonances excited end on—excludes the possibility that the resonances are due to longitudinal "bar" type waves. Finally, we examine in Fig. 14, scattering from a 1.5 to 1 aspect ratio aluminum shell at incident angles of a) end-on, b) 45 degrees relative to axis of symmetry, and c) broadside. Here we can excite three phenomena. At end-on we observe the lowest symmetric Lamb resonances, at 45 degrees we observe in order of occurrence, a bending resonance, the lowest order Lamb resonance excited about the largest meridian, and the two lowest Lamb modes excited about the smallest meridian. Additional bending resonances can be seen weakly at intermediate values. In Fig. 14c we see the broadside results in which the lowest bending

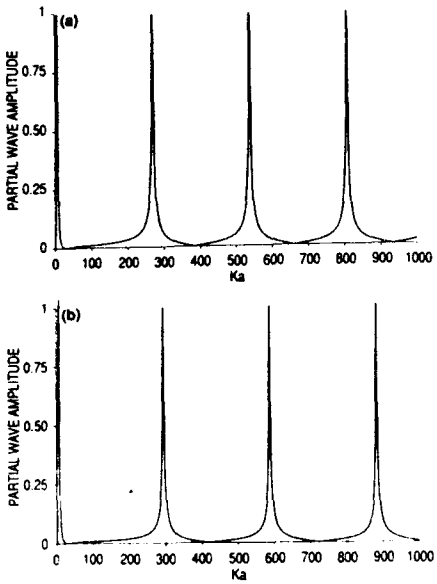

Figure 9. The lowest PWF for a 5% (a) Molybdenum shell; and (b) WC shell to a Ka = 1000.

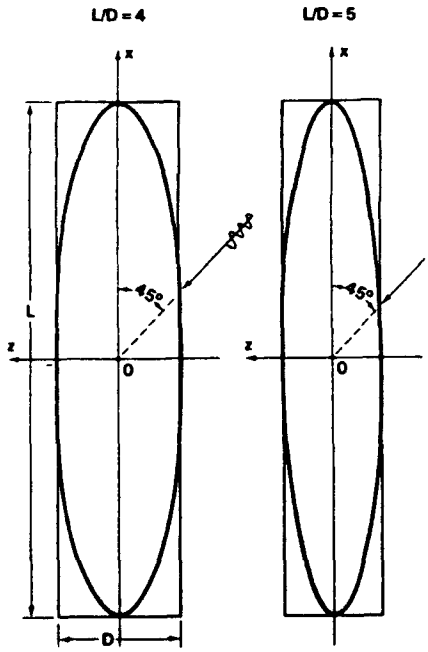

Figure 10. Two of the prolate spheroids and their circumscribed beams.

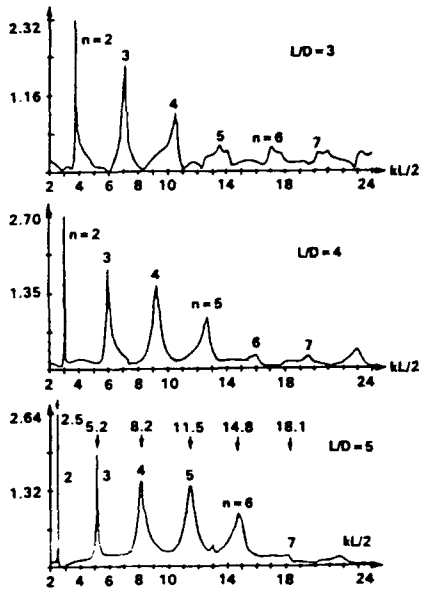

Figure 11. Form-functions, for a steel spheroid in water at 45°.

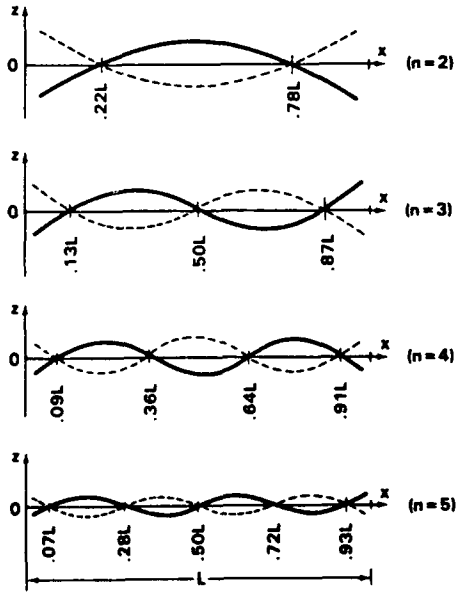

Figure 12. First 4 vibrational modes of a free-free Timoshenko beam (TB).

mode is seen as well as the lowest two Lamb modes about the shortest meridian. What this means is that with the exception of bending modes, an elastic shell (at least of this thickness) has resonances with only two degrees of freedom and that both degrees can be excited at oblique angles (except 90 degrees) and that only the long (short) meridian types can be excited (end-on) broadside. We end this section by giving an approximate expression for predicting the location of bending resonances[16]

$$[kL/2]_{n,s} = \frac{\pi^2}{8\sqrt{2}} \frac{(2n-1)^2}{A_s^2 + \sqrt{A_s^2 + 3\Gamma\pi^2 (n-1)^2/8}} \quad n \geq 2 \qquad (12)$$

where $\Gamma = 2(1+\nu)/K$.

In Eq. (12), K is the shear modulus and A_s is the aspect ratio of the spheroid with the remaining parameters defined below Eq. 9. Figure 15 is a comparison of resonances calculated form the T-matrix (solid curve) and that predicted from Eq. 12. Agreement is quite acceptable.

6. Conclusions

We have illustrated several new large resonance patterns that offer a means of target identification. The case of bending modes are rather narrow which may be difficult to detect in the frequency domain but showed some promise when using the pulse scattering along with gating techniques. The strongest response both in the frequency and the time domain pertains to pseudo-Stonely resonances about the coincidence

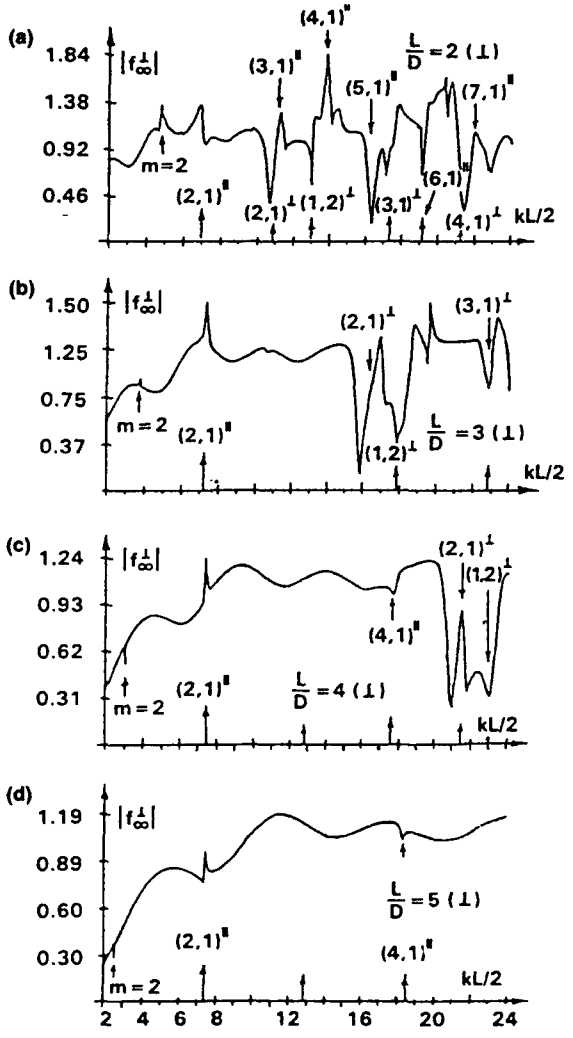

Figure 13. Backscatter from solid steel spheroid broadside incidence for aspect ratio of (a) 2 to 1; (b) 3 to 1; (c) 4 to 1; and (d) 5 to 1 for kL/2 = 2 to 24.

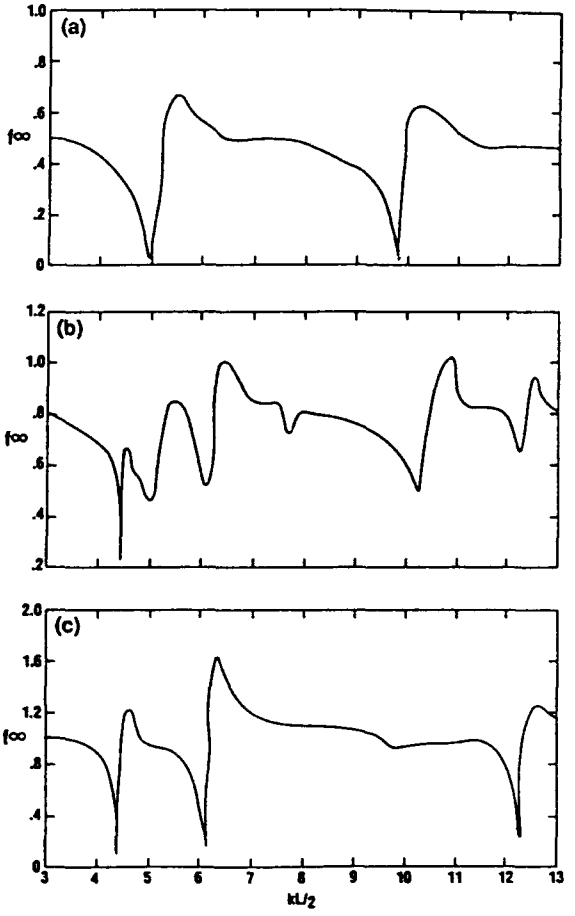

Figure 14. Backscatter from steel spheroid shell of aspect ratio of 1.5 to 1 (a) backscatter; and (b) 45° relative to the axis of symmetry; and (c) broadside.

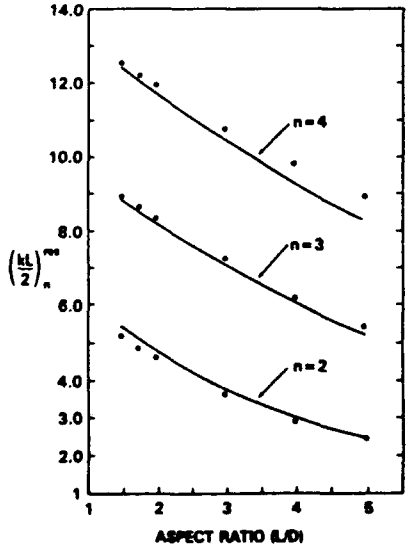

Figure 15. Comparison of two models. Solid line: T-matrix; dots: TB.

frequency region for shells. The location of each of these resonances can be determined by simple expressions (Eqs. 9, 11, and 12).

7. Acknowledgments

We wish to thank the management of the Naval Oceanographic and Atmospheric Research Laboratory and the Office of Naval Research for support of this project. NOARL contribution PR91:100:221.

8. References

1. H. Überall, "Model and surface-wave resonances in acoustic-wave scattering from elastic objects and in elastic-wave scattering from cavities" in *Proceedings of the IUTAM Symposium: Modern Problems in Elastic Wave Propagation*, 1978, Northwestern Univ., Evanston, IL. Sept. 12–15, 1977, edited by J. Miklowitz and J. D. Auchenbach, Wiley Interscience, New York, pp. 239–263.
2. M. F. Werby and L. H. Green, "A comparison of acoustical scattering from fluid loaded elastic shells and sound-soft objects," *J. Acoust. Soc. Am.*, vol. 76, p. 1227, 1984.
3. M. F. Werby and G. C. Gaunaurd, "Transition from soft to rigid behavior in scattering from submerged thin elastic shells," *Acoustics Letters*, vol. 9, No. 7, pp. 89–93, 1986.
4. E. D. Brietenback, H. Überall and K.-B. Yoo, "Resonance acoustic scattering from elastic cylindrical shells," *J. Acoust. Soc. Am.*, vol. 74, p. 1267, 1983.
5. M. C. Junger and D. Feit, *Sound Structures and Their Interaction*. Cambridge, MA: MIT Press, 1972.
6. P. C.Waterman, "New foundation of acoustic scattering," *J. Acoust. Soc. Am.*, vol. 45, p. 1417, 1969.
7. P. C. Waterman, "Matrix formulation of electromagnetic scattering," *Proc. IEEE*, 1965, 53(3), p. 802.
8. P. C. Waterman, "Matrix theory of elastic wave scattering II: a new conservation law," *J. Acoust. Soc. Am.*, vol. 63(6), p. 1320, 1977.
9. M. F. Werby and S. A. Chin-Bing, "Numerical techniques and their use in extension of T-matrix and null-field approaches to scattering," *Int. J. Comp. Math. Appls.*, vol. 11(7/8), p. 717, 1985.
10. M. F. Werby, G. Tango and L. H. Green, "Eigenvalue and similarity transformation methods in the solution of acoustical scattering problems," in *Computational Acoustics: Algorithms and Applications*, D. Lee, R. L. Sternberg, M. H. Schultz (editors) Elsevier Science Publishers B. V. (North Holland), 1988, vol. 2 pp. 257–278.
11. Y.-H. Pao, and V. Varatharajulu, "Huygen's principle, radiation condition, and integral formula for the scattering of elastic waves," *J. Acoust. Soc. Am.*, vol. 60(7), p. 1361, 1976.
12. A. Bostrom, "Scattering of stationary acoustic waves by an elastic obstacle immersed in a fluid," *J. Acoust. Soc. Am.*, vol. 67(2), p. 390, 1980.
13. B. A. Peterson, V. V. Varadan, and V. K. Varadan, "T-matrix approach of study of vibrational frequencies of elastic bodies in fluids," *J. Acoust. Soc. Am.*, vol. 74(5), p. 1051, 1983.
14. M. F. Werby, and L. R. Green, "An extended unitary approach for acoustical scattering from elastic shells immersed in fluids," *J. Acoust. Soc. Am.*, vol. 74(2), pp. 625–632, 1983.
15. M. F. Werby and G. Gaunaurd, "Classification of resonances from scattering at arbitrary incident angles from submerged spheroidal shells", *J. Acoust. Soc. Am.*, vol. 82, pp. 1369–1379, 1987.
16. M. F. Werby and C. G. Gaunaurd, "Flexural resonances in obliquely insonified solid elastic spheroids," *J. Acoust. Soc Am.*, vol. 85, pp. 2365–2371, 1989.
17. L. Flax, G. C. Gaunaurd and H. Überall, "The theory of resonance scattering," in *Physical Acoustics*, 1981, vol. 15, ch. 3 pp. 191–294, W. P. Mason and R. N. Thurston, editors, Academic.
18. J. D. Murphy, J. George, A. Nagl, and H. Überall, "Isolation of resonance component in acoustic scattering from fluid loaded elastic spherical shells," *J. Acoust. Soc. Am.*, vol. 65, p. 368, 1979.
19. M. Talmant, H. Überall, R. D. Miller, M. F. Werby, and J. W. Dickey, "Lamb waves and fluid borne waves on water-loaded, air-filled thin spherical shells," *J. Acoust. Soc. Am.*, vol. 86, pp. 278–289, 1989.
20. G. Quentin, and M. Talmant, "The plane plate model applied to scattering of ultrasonic waves from cylindrical shells," in *Proceedings of the Int. Conf. on Elastic Wave Propagation*, 1989, M. F. McCarthy, and M. A. Hayes, editors, Elsevier Publications B. V., North Holland.
21. M. F. Werby and G. C. Gaunaurd, *J. Acoust. Soc. Am.*, vol. 88, pp. 951–960, 1990.
22. M. F. Werby, "The acoustical background for submerged elastic shells," Submitted. *J. Acoust. Soc. Am.*
23. S. P. Timoshenko, "On the transverse vibrations of beams of uniform cross-section," *Philos. Mag.*, vol. 43, pp. 125–131, 1922.
24. D. Ross, *Mechanics of Underwater Noise*. New York: Pergamon Press, 1976.